

On the deformation of spontaneously twisted fluctuating ribbons

Sergey Panyukov* and Yitzhak Rabin†

*Theoretical department, Lebedev Physics Institute, Russian Academy of Sciences, Moscow 117924, Russia;
and †Department of Physics, Bar-Ilan University, Ramat-Gan 52900, Israel

ABSTRACT A theoretical analysis of the effect of force and torque on spontaneously twisted, fluctuating elastic ribbons is presented. We find that when a filament with a straight center line and a spontaneously twisted noncircular cross section is subjected to a sufficiently strong extensional force, its average elongation exhibits an asymmetric response to large over and under-twist. We construct the stability diagram that describes the buckling transition of such ribbons under the opposing action of force and torque and show that all the predicted behaviors can be understood in terms of continuous transformations between straight and spiral/helical states of the ribbon. The relation between our results and experimental observations on DNA is discussed and a new reentrant spiral to rod transition is predicted at intermediate values of twist rigidity and applied force.

The first experiments on the stretching of double stranded DNA (dsDNA)[1] were successfully described by the wormlike chain model[2, 3] that accounts for the bending rigidity of the molecule. While an extension of this model reproduced the observed bell-shaped curves that characterize the response of dsDNA to torque in the weak stretching regime[4], it could not capture the observed under/overtwist asymmetry at larger applied force[5, 6]. The feeling that linear elasticity alone can not account for the above observations, led to the development of a semi-microscopic theory in which the two strands of the double helix were modeled as elastic filaments connected by rigid rods that represent the base pairs, and an energy penalty was introduced for folding the base pairs with respect to the central axis of the double helix[7]. This theory was able to reproduce most of the experimental observations on the deformation of dsDNA. However, the question is whether one is indeed forced to resort to such microscopic models to account for the experimental findings. In this paper we show that the linear theory of elasticity of spontaneously twisted ribbons combined with statistical mechanics, reproduces the qualitative features of the experiments on stretching and twisting of dsDNA, and provides important insights about the physical origin of the observed phenomena.

1 THE MODEL

The configuration of a thin ribbon of length l and asymmetric cross section is described by a triad of unit vectors $\{\mathbf{t}_i(s)\}$, where s ($0 \leq s \leq l$) is the contour distance, \mathbf{t}_3 is the tangent to the center line and \mathbf{t}_1 and \mathbf{t}_2 are oriented along the principal axes of the cross section. The orientation of the triad as one moves along the filament is given by the solution of the generalized Frenet equations that describe the rotation of the triad vectors, $\mathbf{t}'_i(s) = \sum_{j,k} \varepsilon_{ijk} \omega_j(s) \mathbf{t}_k(s)$, where ε_{ijk} is the antisymmetric tensor, the prime denotes differentiation with respect to s ($\mathbf{t}'_i = d\mathbf{t}_i/ds$), and $\{\omega_i(s)\}$ are the curvature and torsion parameters[8]. These equations can be rewritten in terms of the Euler angles θ, φ and ψ :

$$\begin{aligned} \theta' &= \omega_1 \sin \psi + \omega_2 \cos \psi, \\ \varphi' \sin \theta &= -\omega_1 \cos \psi + \omega_2 \sin \psi, \\ \psi' \sin \theta &= (\omega_1 \cos \psi - \omega_2 \sin \psi) \cos \theta + \omega_3 \sin \theta. \end{aligned} \quad (1)$$

Notice that while the angles $\theta(s)$ and $\varphi(s)$ describe the spatial conformation of the center line, $\psi(s)$ describes the rotation of the cross section about this center line.

The elastic energy of a deformed ribbon is given by the sum of bending and twist contributions, $U_{el} = U_{bend} + U_{twist}$ where[8]

$$\begin{aligned} U_{bend} &= \frac{kT}{2} \int_0^l ds (a_1 \omega_1^2 + a_2 \omega_2^2), \\ U_{twist} &= \frac{kT}{2} a_3 \int_0^l ds (\omega_3 - \omega_{30})^2 \end{aligned} \quad (2)$$

Here k is the Boltzmann constant, T is the temperature, the bare persistence lengths a_1 and a_2 represent the bending rigidities with respect to the two principal axes of inertia of the cross section, and a_3 is associated with twist rigidity. We assume that the stress-free reference state corresponds to a ribbon with a straight center line oriented along the x -axis and a cross section that is twisted about this line at a rate ω_{30} (this defines the twist number in $T\omega_0 = l\omega_{30}/2\pi$ and the total angle of twist $l\omega_{30}$). The above expression for the energy is based on linear theory of elasticity and applies to deformations whose characteristic length scale is much larger than the diameter of the filament[9]. Since we consider the deformation of the ribbon by forces applied to its ends, the total energy contains an additional term $-(kTf/l) \int_0^l ds \sin \theta \cos \varphi$ where

f is the force in units of kT/l . This theory is a generalization of the wormlike chain model[2] to the case of a ribbon with noncircular cross section and nonvanishing spontaneous twist.

In this work we only consider small deviations of the Euler angles $\delta\theta$, $\delta\varphi$ from their values $\theta_0 = \pi/2$, $\varphi_0 = 0$ in the stress-free state. Physically, this corresponds to the strong force regime, $f \gg 1$, in which the tangent vector $\mathbf{t}_3(s)$ undergoes only small fluctuations about the x axis. No restrictions on the magnitude of the deviation $\delta\psi$ from the spontaneous value $\psi_0(s) = \omega_3 s$ are imposed. Expanding the energy to second order in the deviations $\delta\theta$, $\delta\varphi$ and introducing the complex variable $\Phi = [\delta\theta + i\delta\varphi]e^{-i\psi}$ yields

$$\frac{U}{kT} = -f + \int_0^l ds \left\{ \frac{f}{2l} |\Phi|^2 + \frac{a_1 + a_2}{4} |\dot{\Phi}|^2 + \frac{a_2 - a_1}{8} \left[\dot{\Phi}^2 + (\dot{\Phi}^*)^2 \right] \right\} + \frac{U_{twist}}{kT}, \quad (3)$$

where we defined $\dot{\Phi} = \Phi' + i\psi'\Phi$, and where $\omega_3 = \psi' + \frac{i}{4}(\Phi^*\dot{\Phi} - \Phi\dot{\Phi}^*)$.

We proceed to calculate the free energy of the deformed ribbon, for a given value of the total angle of twist, $\psi(s) = \psi's$, where we assume that rate of change ψ' is constant (a priori, we do not exclude the possibility that solutions with different values of this constant coexist in the filament). The constrained partition function is evaluated by carrying out the functional integrals over Φ , Φ^* with the Boltzmann weight $\exp(-U/kT)$. Since U_{twist} contains quartic terms in these fields, in order to calculate the integrals over Φ and Φ^* we introduce the Hubbard-Stratonovitch transformation of the twist contribution to the partition function

$$\exp(-U_{twist}/kT) = \int D\gamma(s) \times \exp \int_0^l ds \left[\frac{\gamma^2}{2(2\pi)^2 a_3} - \frac{\gamma}{2\pi} (\omega_3 - \omega_{30}) \right] \quad (4)$$

where γ can be interpreted as a fluctuating torque. The resulting free energy is a quadratic form in Φ and Φ^* and the Gaussian integrals over these fields can be carried out exactly. For convenience, we assume that the field $\Phi(s)$ obeys periodic boundary conditions, $\Phi(L) = \Phi(0)$, and diagonalize the free energy by expanding $\Phi(s)$ in Fourier series, $\Phi(s) = \sum_n \tilde{\Phi}_n e^{i2\pi ns/L}$. A different choice of boundary conditions would affect our results only in the weak force region (in this work we will only consider the range $f \gg 1$). The integral over γ is calculated by the steepest descent method. This yields the free energy

$$\frac{\mathcal{F}(f, \gamma)}{kT} = -f + \gamma(Lk - Tw_0) - \frac{\gamma^2}{2C} + \frac{1}{2} \sum_{n=-\infty}^{\infty} \ln h_n(f, \gamma) \quad (5)$$

where we defined $Lk = \psi(l)/2\pi$ and where $h_n(f, \gamma) = f^2 + 2f[B(n^2 + Lk^2) - \gamma Lk] + (n^2 - Lk^2)[A^2(n^2 - Lk^2)$

$+ 2B\gamma Lk - \gamma^2]$ with $A = (2\pi)^2 \sqrt{a_1 a_2}/l$, $B = (2\pi)^2(a_1 + a_2)/2l$ and $C = (2\pi)^2 a_3/l$. A relation between Lk and the torque γ is obtained by minimizing the free energy with respect to γ :

$$Lk = Tw_0 + \frac{\gamma}{C} + \sum_{n=-\infty}^{\infty} \frac{(n^2 - Lk^2)(\gamma - BLk) + Lkf}{h_n(f, \gamma)}. \quad (6)$$

This relation has a simple geometrical meaning. The twist number $Tw = (1/2\pi) \int_0^l ds \omega_3(s)$ can be related to the torque γ by steepest descent evaluation of the integral in Eq. (4) that yields $Tw = Tw_0 + \gamma/C$. Inverting Eq. (1) and assuming $|\delta\theta| \ll 1$, the twist number can be written as $Tw = (1/2\pi) \int_0^l ds [\psi' - \delta\theta d(\delta\varphi)/ds]$. For $|\delta\theta| \ll 1$ the writhe number can be expressed as [4] $Wr = (1/2\pi) \int_0^l ds \delta\theta d(\delta\varphi)/ds$ and thus $Tw + Wr = \psi(l)/2\pi$. Since the sum of twist and writhe numbers is the linking number [10], we conclude that our definition of Lk coincides with the standard definition of the linking number. Inspection of Eq. (6) shows that the first two terms on the rhs of this equation give the twist number and that the third term is the writhe number.

A quantity that can be readily measured in experiments is the mean elongation of the filament (average end to end distance), $\langle R \rangle = -(l/kT) \partial \mathcal{F} / \partial f$. The dependence of the elongation on the total angle of twist ($2\pi Lk$) and on the extensional force is studied below.

2 RESULTS

Effect of torque on elongation. In Fig. 1 we plot the average elongation $\langle R \rangle$ vs. the linking number, for a spontaneously twisted ribbon ($Lk_0 = Tw_0 = 10$, $A = C = 10$, $B = 50$). At relatively low values of the force, we obtain a symmetric bell-shaped curve (curve a), in agreement with reference [4]. Notice that fluctuations shift the peak of the curve to $Lk_{\max} \simeq 9.4$ which is somewhat smaller than the spontaneous value. As f is increased, the dependence of the elongation on the angle of twist becomes progressively asymmetric (curve b); $\langle R \rangle$ decreases linearly with overtwist but is nearly independent of undertwist throughout the range $0 \lesssim Lk \lesssim Lk_0$. At yet higher values of f , the elongation becomes nearly independent of under or overtwist, in a broad range of linking numbers (curve c).

In order to understand how the average conformation of the filament varies with the linking number, in the insert to Fig. 1 we plot the torque γ and the twist number Tw vs. Lk , for a value of f that corresponds to curve b in this figure. Both γ and Tw increase linearly with Lk in the range that corresponds to the flat portion of curve b, and approach constant values in the range where linear decrease of elongation with degree of over or undertwist is observed. In the range where Tw increases linearly with Lk (see insert), the writhe number remains

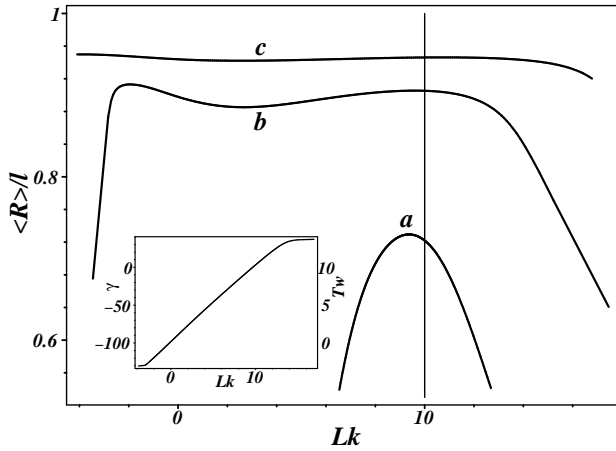


Figure 1: The average normalized elongation $\langle R \rangle / l$ is plotted vs the linking number Lk , for a ribbon with $Lk_0 = 10$, $A = 10$, $B = 50$ and $C = 10$ ($a_1 \simeq 1$, $a_2 \simeq 100$ and $a_3 = 10$). The extensional force corresponding to the three curves are a) $f = 50$, b) $f = 350$ and c) $f = 1000$. The dependence of the torque (twist) on the linking number for $f = 350$ is shown in the insert.

small and the application of torque to the ends of a rectilinear filament results mainly in twist of its cross section about a straight center line. At large values of overtwist ($\Delta Lk = Lk - Lk_{\max} > 0$) for which Tw approaches a constant value, further increase of the linking number leads to the appearance of large mean writhe and the filament undergoes a transition to a spiral or a helical configuration. As will be shown in the following, this transition is related to buckling of elastic rods under torque[9] (in the presence of thermal fluctuations the buckling instability is replaced by a continuous change of shape with increasing torque). Further increase of Lk increases both the amplitude (the radius) and the number of turns of the spiral and leads to progressive shortening of the average length of the filament, in agreement with the behavior observed in Fig. 1b. Inspection of the insert shows that linear variation of Tw with Lk takes place over much broader range of undertwist than of overtwist, indicating that throughout the plateau region in Fig. 1b, the removal of spontaneous twist takes place mainly by untwisting a straight filament, leaving $\langle R \rangle$ unaffected. The shallow minimum in the plateau region of curve b is related to the existence of a reentrant spiral/helix to rod transition that will be discussed below.

Force versus elongation. In Figs. 2a and 2b we plot f vs. $\langle R \rangle$ for different values of Lk corresponding to undertwist and overtwist, respectively. For small deviations from Lk_0 , the curves are symmetric under $\Delta Lk \leftrightarrow -\Delta Lk$. For larger deviations a plateau-like region is observed at intermediate elongations, that is reached more rapidly for undertwist than for overtwist. Since for each set of parameters we find a unique solution ψ' of Eq. (6), the above plateau is not associated with coexistence of two phases. Rather, the observation of a

region of nearly constant $\log f$ over a large range of elongations means that in this region of parameters f varies slower than exponentially with $\langle R \rangle$ (e.g., as a power).

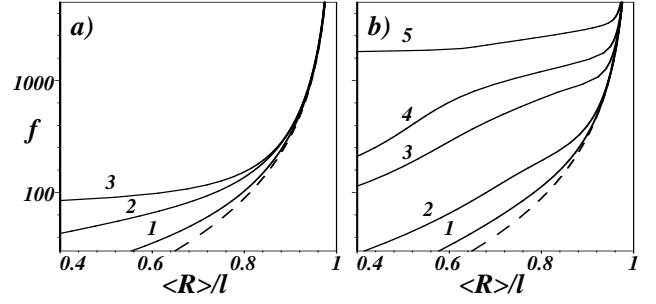


Figure 2: a) Plot of f vs. $\langle R \rangle / l$, for increasing degrees of undertwist. The broken line corresponds to a spontaneously twisted ribbon ($Lk = Lk_0$), and curves 1 – 3 to $\Delta Lk = -1.5, -3$ and -10 , respectively. b) Plot of f vs. $\langle R \rangle / l$ for increasing degrees of overtwist. The broken line corresponds to $Lk = Lk_0$, and curves 1 – 5 to $\Delta Lk = 1.5, 3, 7, 10$ and 15 , respectively. All elastic parameters are as in Fig. 1.

Buckling under torque. The simple physical picture behind the above observations is intimately related to the well-known buckling transition under torque and, in order to gain intuition about the different parameter ranges, we examine the stability of the straight filament under the combined action of tension and torque. We substitute Eq. (4) into $\exp(-U/kT)$ and look for the conditions under which the quadratic form in Φ is no longer positive definite. In the absence of thermal fluctuations, a straight filament becomes unstable against buckling under torque at $h_n(f, \gamma) = 0$. The shape of the filament following buckling is given by a combination of Fourier modes $\tilde{\Phi}_n$ and $\tilde{\Phi}_{-n}$, where n is found by minimizing $h_n(f, \gamma)$ with respect to n . In the presence of thermal fluctuations $h_n(f, \gamma) > 0$ everywhere and the buckling instability is replaced by a continuous deformation of the mean conformation of the filament from a straight line into a three-dimensional curve. In the limit of strong force and torque (the regime in which $\langle R \rangle$ decreases linearly with Lk —see curve b in Fig. 1), the resulting shape is dominated by a combination of modes with wave vectors $2\pi(Lk \pm n)/l$. The case $n = 0$ corresponds to a simple helix with period l/Lk and the smaller axis of inertia of the cross section (direction of easy bending) rotating in the plane normal to its symmetry axis (see Fig. 3).

In Fig. 3 we plot the line of buckling transitions in the $f - Lk$ plane for the same elastic parameters as in the preceding figures. The thick portions of the solid line correspond to instability at $n = 0$ (rod to helix transition) and the thin portion of the line corresponds to $n \neq 0$ (rod to spiral transition). The four inserts describe the average configuration of the ribbon, at the locations shown by the corresponding arrows on the stability diagram. Insert 1 describes a ribbon with a cross section sponta-

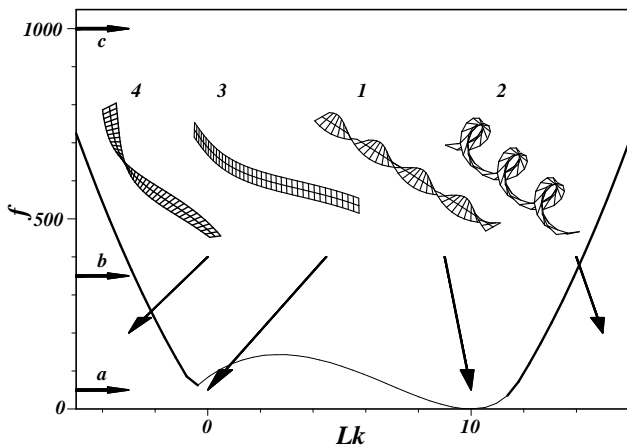


Figure 3: The stability diagram in f vs Lk plane, for elastic ribbon with the same parameters as in Fig. 1 (the straight twisted ribbon configuration is stable against buckling above this line). The configurations of the filament in different regions of the diagram indicated by the arrows are shown in inserts 1 – 4. The arrows denoted by a, b and c on the lefthand side of the figure correspond to the appropriate curves in Fig. 1.

neously twisted about a straight center line (no applied torque), and corresponds to the stable region above the minimum at $Lk = Lk_0$. Insert 2 corresponds to the unstable region to the right of this minimum (overtwist), in which buckling transforms the straight twisted ribbon into a helix, with the smaller moment of inertia of its cross section oriented normal to the axis of symmetry of the helix. The origin of the broad symmetric minimum at $Lk = Lk_0$ is intuitively clear—small over/undertwist with respect to the equilibrium configuration destabilizes the filament against buckling and a larger extensional force is needed to maintain the straight state. The fact that in the absence of torque the instability appears to take place at $f \rightarrow 0$ rather at some negative value of the stretching force corresponding to the Euler instability under load, is a consequence of our periodic boundary conditions; since the ends of the filament are not fixed, for $f \rightarrow 0$ there is an instability against rigid rotation of the filament. The smaller minimum at $Lk \simeq 0$ appears only in the presence of large spontaneous twist ($Lk \gg 1$) and bending asymmetry ($a_1, a_3 \ll a_2$). Insert 3 shows a typical configuration in the unstable region just below this minimum – buckling produces an untwisted ribbon bent along its easy axis. Since the stretching of this filament is opposed only by the smaller of the bending rigidities, it can be easily stretched into a straight configuration. The presence of even small deviations from $Lk = 0$ creates a nonplanar configuration shown in insert 4, the stretching of which invokes both the easy (a_1) and the hard (a_2) bending axes, and requires a larger extensional force (hence the minimum).

The arrows a, b, c on the left hand side of Fig. 3 refer to the corresponding curves in Fig. 1. Recall that while thermal fluctuations were neglected in the deriva-

tion of the stability diagram in Fig. 3, they were included in the calculations leading to Fig. 1 (their main effect is to broaden the stability line into an extended transition region between straight and spiral/helical states of the ribbon). Case (a) corresponds to the weak force regime in which strong fluctuations smear out the stability curve in the vicinity of the minimum at $Lk = Lk_0$, resulting in a symmetric bell-shaped curve (see Fig. 1). Cases (b) and (c) correspond to the strong force regime. For small overtwists, all excess linking number goes into pure twist and the filament maintains (on the average) its straight configuration. At larger linking numbers beyond the fluctuation-broadened stability line, the filament develops positive writhe and undergoes a continuous rod-to-helix transition. Further increase of Lk increases the radius and number of turns of the helix, resulting in a linear decrease of $\langle R \rangle$. When the ribbon is subjected to undertwist, the filament remains straight and “unwinds” over a much larger range of undertwist compared to overtwist (because of the pronounced asymmetry of the stability line), giving rise to the plateau regions in curves b and c, in Fig. 1. Note that there is an intermediate regime between cases (a) and (b), in which undertwist leads to reentrant behavior. For small degrees of undertwist, decreasing Lk initially unwinds the spontaneously twisted but straight filament and, as the stability line is crossed for the first time, the ribbon deforms into a helix with negative writhe and $\langle R \rangle$ decreases with increasing undertwist. As the stability line emanating from the $Lk = 0$ minimum is approached, the helix undergoes a reentrant transition into an untwisted rod and $\langle R \rangle$ increases (a trace of this behavior is evident in curve b of Fig. 1). Finally, at yet higher undertwists the stability line is crossed again and a transformation into a negatively twisted spiral takes place, accompanied by rapid decrease of $\langle R \rangle$.

3 DISCUSSION

In this paper we studied the response of spontaneously twisted fluctuating elastic ribbons to externally applied torque and extensional force. The analysis is based on a combination of linear theory of elasticity and statistical mechanics, and the only input from an underlying microscopic level of description is contained in the values of the elastic constants and of the rate of spontaneous twist. The agreement between our results and those of reference [7], is not surprising since the linear theory of elasticity is the long wavelength limit of any physically reasonable microscopic theory of solid behavior. Even though we made no effort to adjust our model parameters to fit dsDNA[11], our Figs. 1 and 2 contain most of the qualitative features of the experimental observations on twisted and stretched DNA in the intermediate range of force, 1 – 70 pN[5, 6]. An exception to this statement is the predicted rapid decrease of elongation in the limit of large undertwist (Fig. 1b) that was not observed

in experiment, possibly because the predicted decrease in elongation is preempted by a microscopic structural transition of dsDNA (alternatively, the decrease in elongation may occur at yet larger degrees of undertwist not reached in the experiments).

All the features observed in Figs. 1 and 2 can be understood in terms of a simple physical picture based on the stability diagram, Fig. 3, that describes the buckling instability under the opposing actions of torque and extensional force. When torque is applied to a straight spontaneously twisted ribbon, its response depends on the direction of the torque relative to that of spontaneous twist, and on the magnitude of f (assumed to be fixed during the process). For small degrees of overtwist, the filament remains straight and its cross section is twisted in excess of the spontaneous value. As the transition region around the stability line is reached, the straight ribbon deforms into a spiral curve or into a helix, depending on f . When the ribbon is subjected to undertwist it unwinds while maintaining a straight center line over much larger range than in the case of overtwist. Eventually, the transition region is reached and the straight ribbon deforms into a spiral or a helix. For the range of elastic parameters studied in this paper ($a_1 \ll a_3 \ll a_2$) the stability diagram contains an additional minimum at $Lk \simeq 0$ and, for small enough f , further undertwist leads to a spiral to rod transition (for forces below the critical value corresponding to this minimum the spiral transforms into a periodically bent planar configuration). At yet higher degrees of undertwist the straight filament deforms again into a helix. For larger values of f (above the value at the local maximum at $Lk \simeq 3$ in Fig. 3), the application of undertwist leads to the untwisting of a straight filament, resulting in a broad plateau in $\langle R \rangle$. Such behavior was observed both in experiments on dsDNA[5, 6] and in our Fig. 1. Note that although the value of f corresponding to curve b in Fig. 1 is well above the local maximum of the stability line of Fig. 3, the nonmonotonic variation of $\langle R \rangle$ with degree of undertwist suggests that the fluctuations of the filament (and hence its elongation) are affected by the presence of the minimum at $Lk \simeq 0$. While there is no compelling experimental evidence for reentrant behavior in dsDNA to date (however, a shallow minimum in $\langle R \rangle$ at intermediate values of f , is clearly visible in Fig. 3 of reference [5]), it will be interesting to look for it in other systems such as dsDNA “dressed” by attached proteins, RNA, etc..

We would like to comment on the possible ramifications of this work. Both the strength and the limitation of the present approach are its generality – while the description of the deformation of spontaneously twisted ribbons is a hitherto unsolved problem that is interesting in its own right, one may question whether it is a suitable model for dsDNA. Thus, one may ask whether the large asymmetry of the bending persistence lengths ($a_2/a_1 \simeq 100$) necessary to produce the curves in Figs. 1–3 is physically reasonable. In order to answer this question notice that if we model a double helix by a sponta-

neously twisted ribbon, the bending coefficients of this ribbon correspond to a hypothetical untwisted state of dsDNA in which two strands connected by base pairs form a ladder-like structure (two multiply connected, straight parallel lines). Such a structure is expected to have large asymmetry for bending in the plane of the ladder (a_2) or normal to it (a_1) (dsDNA was modelled as a ribbon polymer made of two semi-flexible chains that could not be bent in the plane of the ribbon, in reference [12]). The effective persistence length a_{eff} of our model is given by the relation $a_{eff}^{-1} = (a_1^{-1} + a_2^{-1})/2$ and approaches $2a_1$ in the limit $a_2 \gg a_1$ (thus, while $a_1 \simeq 25$ nm is determined by the persistence length of dsDNA, a_2 has no direct physical interpretation).

Another issue involves the description of deformation-induced internal transitions in dsDNA invoked by experimenters[13] in order to explain the observed plateau in plots of f vs. $\langle R \rangle$, as well as the observed opening of the DNA bases at large undertwists (by hybridization with complementary fragments), and the increased reactivity of some bases at large overtwists. Even though in our continuum elastic model, there is no direct reference to internal structure, analogies between shape changes and structural transitions can be readily drawn. Thus, variations of internal structure would correspond to changes of the average conformation of the filament and it is plausible that the conformations shown (see inserts 1 – 4) in Fig. 3 differ in their chemical reactivity, consistent with the observations of reference [13]. Furthermore, the experimental observation that even relatively small undertwists lead to denaturation[13], is consistent with our result that over a large range of undertwists, the cross section unwinds around a straight center line and no writhe develops (one expects twist around a center line to be more effective than writhe of the center line in disrupting the interaction between the base pairs). A deeper difference between our discussion of force and torque induced shape changes and that of transitions between different internal states of dsDNA in reference [13] is that while we find only continuous transformations of average conformation, discontinuous first order internal transitions (from B to P and S forms) and phase coexistence are invoked in the latter work.

Since our model assumes small deviations of the Euler angles from their stress-free values, it can not describe large amplitude defects (with $\delta\theta, \delta\varphi \gtrsim \pi$) such as plectonemes. However, our analysis shows that for $f \gg 1$, the formation of plectonemes is preempted by the appearance of homogeneous spiral and helical structures (recall that the classical torsional buckling instability corresponds to a transition to a helical state with arbitrarily small amplitude[9]), even though plectonemes may appear at yet larger applied torques. Finally, the fundamental limitation of our theory is that since it is based on the linear theory of elasticity of thin inextensible rods, it can not describe the observed overstretching of B-DNA by 1.7 times its native length[14, 15], and one must resort to microscopic[7] or thermodynamic[16] ap-

proaches.

We would like to thank David Bensimon and M. Elbaum for helpful comments on the manuscript. YR acknowledges support by a grant from the Israel Science Foundation.

References

- [1] Smith S.B., Finzi, L. and Bustamante, C. (1992) *Science* **258**, 1122.
- [2] Marko, J.F. and Siggia, E.D. (1994) *Macromolecules* **27**, 981 .
- [3] Bustamante, C., Marko, J.F., Siggia, E.D. and Smith, S.B. (1994) *Science* **265**, 1599.
- [4] Bouchiat C. and Mezard, M. (1998) *Phys. Rev. Lett.* **80**, 1556; (2000) *Eur. Phys. J. E* **2**, 377.
- [5] Strick, T.R., Allemand, J.-F., Bensimon D., Bensimon A. and Croquette V. (1996) *Science* **271**, 1835.
- [6] Strick, T.R., Croquette, V. and Bensimon, D. (1998) *Proc. Natl. Acad. Sci.* **95**, 10579.
- [7] Zhou, H.J., Zhang, Y. and Ou-Yang, ZC. (1999) *Phys. Rev. Lett.* **82**, 4560; (2000) *Phys. Rev. E* **62**, 1045.
- [8] Panyukov, S. and Rabin, Y. (2000) *Phys. Rev. Lett.* **85**, 2404; (2000) *Phys. Rev. E* **62**, 7135.
- [9] Love, A.E.H. (1944) *A Treatise on the Mathematical Theory of Elasticity* (Dover, New York).
- [10] White, J. H. (1969) *Am. J. Math.* **91**, 693.
- [11] In making the comparison one should use the force F and the degree of supercoiling $\Delta Lk/Lk_0$, that do not depend of the length of the filament.
- [12] Golestanian R. and Liverpool, T.B. (2000) *Phys. Rev. E* **62**, 5488.
- [13] Strick, T.R., Allemand, J.-F., Bensimon D., Lavery R. and Croquette V. (1999) *Physica A* **263**, 392.
- [14] Cluzel, P., Lebrun, A., Heller, C., Lavery, R., Viovy, J.-L., Chateney, D. and Caron, F. (1996) *Science* **271**, 792.
- [15] Smith, S.B., Cui, Y. and Bustamante, C. (1996) *Science* **271**, 795.
- [16] Rouzina, I. and Bloomfield, V.A. (2001) *Biophys. J.* **80**, 882.